

Observation of Ultra Low Hard X-ray Flux from Cyg X-1 – A Possible Partial Occultation of the X-ray Source

R. K. Manchanda *

Tata Institute of Fundamental Research, Colaba, Mumbai - 400 005, India

Received 2000 June 1; accepted 2000 September 5.

Abstract. The black hole candidate Cyg X-1 was observed in ultra low state on March 30, 1997 using Large Area Scintillation counter Experiment (LASE) in the hard X-ray energy region of 20–180 keV. During the 30 minute exposure a combined signal of 68 sigma was obtained, however, the measured flux at 50 keV was lower by a factor of 2 than the minimum flux reported so far. Using the recent orbital ephemeris of the source, our snap-shot observations were made at $\phi_{5.6} = 0.915$, which corresponds to the binary minimum revealed by the ASM light curves. The daily average data from the BATSE detectors give the source intensity level to be higher by a factor of 5. Very low flux values measured in the present experiment suggest that the hard X-ray source may have been partially occulted by the primary companion during its transit near the X-ray minimum.

Key words: Accretion, accretion disks – X-rays: stars – black hole candidate: individual– Cyg X-1.

1. Introduction

Cyg X-1 is the brightest X-ray binary source in the hard X-ray and soft gamma ray energy region to date, and is the best candidate for stellar mass black holes. In spite of extensive studies during the last 35 years, the X-ray source still remains enigmatic. Apart from the 5.6^d binary orbital period (Dolan *et al.* 1979), the source also exhibits a 294^d periodicity (Manchanda 1983, Priedhorsky *et al.* 1983, Kemp *et al.* 1983, Kemp *et al.* 1987). Intensity variability down to millisecond time scales, and chaotic rapid variations have been observed from the source. Spectral variability in hard X-rays on time scales of minutes has been reported in the literature (Tanaka & Lewin 1995 and references therein).

The source shows two distinct spectral states, ‘X-ray low’ and ‘X-ray high’,

*e-mail:ravi@tifr.res.in

depending on the low energy flux below 10 keV and the power law index changes from 1.5 to $\sim 3 - 4$ between the two states. During its low state, the X-ray spectrum is dominated by photons up to several hundred keV. However, the HEAO-C observations during September 1979 to July 1980 revealed the presence of a 'super-low' state in which both the soft X-ray and hard X-ray flux dropped simultaneously (Ling *et al.* 1983). Three distinct intensity levels namely 'X-ray low' (γ_1), 'X-ray high' (γ_2) and 'X-ray very high' (γ_3), have been suggested on the basis of the power density spectrum analysis (PDS) of the source intensity and the strength of the quasi-periodic oscillations (Tanaka 1989; van der Klis 1995). Cyg X-1 went through an extended low luminosity level (γ_0) in 1994 during which the 45–140 keV flux decreased to almost 25% of the normal X-ray high state value (Ling *et al.* 1997). Discrete intensity states for source is a simplified description for deriving the model parameters, the BATSE light curve of the daily averaged intensity suggests a continuous luminosity variation of the source.

The binary period of 5.6^d for the source has been established from the optical observations and the X-ray sinusoidal binary light curve has been recently observed from the RXTE data (Pooley *et al.* 1999). No clear dip due to the eclipsing by the primary companion has been seen either in the optical data or the soft X-ray light curve. Cygnus X-1 is also one of the most variable high energy source, and no systematic spectral studies at high energies with its binary phase have been made so far. The model fitting for the broad band X-ray spectrum of the source itself has been a matter of great debate. While the low energy components are modeled with galactic absorption for a black body input spectrum with a K_{α} fluorescence emission line due to Iron at 6.7 keV, high energy continuum has been fitted both with Comptonized power law, addition of a reflection component and two component Comptonized spectra (Chitnis *et al.* 1998).

The snap-shot X-ray spectrum obtained during the present experiment is much steeper than the canonical power index $\alpha \sim 2$, suggestive of the 'mid' or 'low' state. The total luminosity of the source was also found to be lower by a factor of about 2 compared to the measurements even during the super low state. Since the present observations correspond to the minimum in binary light curve as seen in the ASM phase data, and the daily averaged intensity of the source in the 45–150 keV energy band on the day of our observation was by a factor of 5 higher (BATSE archival data), the present observations suggest a partial eclipsing of the hard X-ray emission region of the source near the minimum phase. The source spectrum has a peculiar knee-shaped profile and we discuss the physical conditions, which can lead to this behaviour.

2. Experimental details

The observations were made with a Large Area Scintillation counter Experiment (LASE) which is designed to study fast variations in the flux of X-ray sources in the hard X-ray energy region up to 200 keV. The payload consists of three large area

X-ray detector modules mounted on a servo-controlled platform. The detectors are a specially designed combination of thin and thick large area NaI(Tl) scintillation counters configured in back-to-back geometry. Each of the detector modules has a geometrical area of 400 cm^2 and the thickness of the prime detector is 3mm. The active anti-coincidence shield is provided by a 30 mm thick crystal. The field of view of each module is $4.5^\circ \times 4.5^\circ$ and is defined by demountable mechanical slat collimator specially designed with a sandwiched material of lead, tin and copper. Each module along with the collimator is further encased with a passive shield. Each detector is designed as a stand-alone unit with independent on-board subsystems for HV power and data processing. LASE payload is fully automatic with an on-board star tracker and requires no ground control during the flight. The detector modules have 100% detection efficiency in the operative energy region and the back-to-back configuration gives 80% reduction in the detector background. The details of the detector design, associated electronics, control sub-systems and the in-flight behaviour of the instrument are presented elsewhere (D'Silva *et al.* 1998). The response matrix of each detector was constructed from the pre flight calibration of the detectors at different X-ray line energies using a variety of radioactive sources Am^{241} (24.7 keV and 59.6 keV), Ba^{133} (32.4 keV and 81 keV), Cd^{109} (22.1 keV and 97.5 keV). To calibrate the high energy end of chosen energy range, we used highly accurate 'divide by two' attenuators in the detector outputs and observed the 300 keV and 357 keV lines from Ba^{133} . In addition, an Am^{241} source is mounted on the payload for periodic calibration of the payload by command during the flight. Accepted events from various detectors are pulse height analyzed and time tagged with 25 μsec resolution and are transmitted to the ground on a 40 kbit PCM/FM link. The 3σ sensitivity of the LASE telescope in the entire energy range up to 180 keV is $\sim 1.5 \times 10^{-6} \text{ cm}^{-2} \text{ s}^{-1} \text{ keV}^{-1}$ for a source observation of 10^4 sec.

The balloon flight was launched on 30 March 1997 from Hyderabad, India (cut-off rigidity 16.8 GV) and reached a ceiling altitude of 3.3 mbs. A number of X-ray sources Her X-1, GR 1744-28, GS 1843+00, GRS 1905+105, Cyg X-1 and Cyg X-3 were observed during the experiment. Cyg X-1 was in the field of view of the two detectors for a total period of 30 minutes during 0530 to 0600 UT. The background was derived from two observations of a blank field before and after the source pointing. The present observation of the source corresponds to MJD 50536.07.

3. Results and Discussion

The counting rate profile from the two detectors during the source observation is shown in Fig. 1. The data are plotted as the total counts in the entire energy band versus bin number ($\sim 30\text{sec}$) for each detector. The top panel gives the azimuthal information about the source acquisition and the tracking during the observation. The source observation interval is marked by the arrows. It is clearly seen from

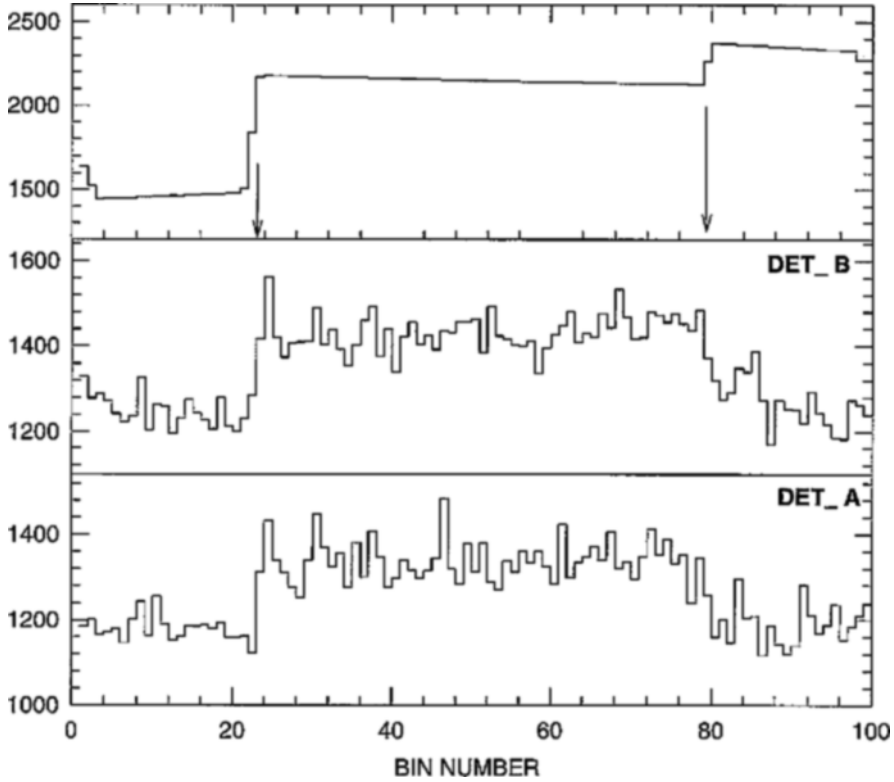


Figure 1. The counting rate profile of the two detectors during the observation of Cyg X-1. The top panel gives the target tracking and is marked by arrows. The bin size is ~ 30 sec. Y-axis gives the integral counts for the detectors and azimuth shaft-encoder value for the upper panel.

the figure that the observed counting rate registered a significant increase as soon as the detectors acquired the target and an excess of $\sim 6 \text{ ct. s}^{-1}$ was recorded due to the source. A total excess of 11070 and 12750 counts was obtained in each of the two detectors and corresponds to a combined statistical significance of 68σ in the 20–180keV energy band. The source contribution was divided in 16 energy bins and corrected for the atmospheric absorption of 3.3 mbs corresponding to the float altitude, window transmission, detection efficiency and the energy resolution of each detector. An additional correction of 10% due to the systematic effects was applied to data below 26 keV.

The combined deconvolved hard X-ray spectrum of the source is shown in Fig. 2. The observed spectra of the source obtained during ‘X-ray low/hard’ (γ_1), ‘X-ray high/soft’ (γ_2) and super low state (γ_0) are also plotted in the figure for comparison. The high state spectrum is taken from the HEXTE data on board RXTE satellite

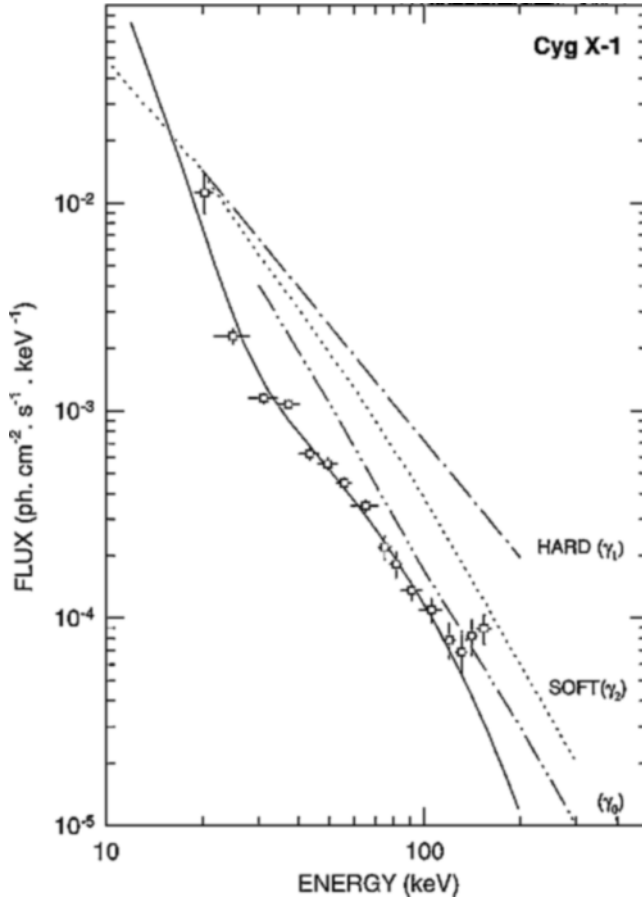


Figure 2. Hard X-ray spectrum of Cyg X-1. ‘X-ray high/soft’, ‘X-ray low/hard’ and super low state spectra are shown for comparison. Solid line represents a two temperature thermal fit.

(Cui *et al.* 1998). The low state spectrum (Ubertini *et al.* 1991, Ling *et al.* 1997) and super low state data corresponds to Ling *et al.* (1997) and Philips *et al.* (1996). It is seen from the figure that the present data show a peculiar knee-shaped spectral profile and is quite different from the observations made so far. It is interesting to note that the low energy point compares well with the other data while the data above 30 keV are a factor of $\sim 5-7$ lower than the high state spectrum and a factor of 2 lower than the super low state. In order to further establish that the observed features in the spectrum of Cyg X-1 are genuine and that there was no other unknown systematic effect, we have plotted the observed spectrum of Cyg X-3 in Fig. 3, which was tracked after Cyg X-1. The data of Rao *et al.* (1991) obtained using a xenon filled proportional counter telescope are also shown for comparison. It is

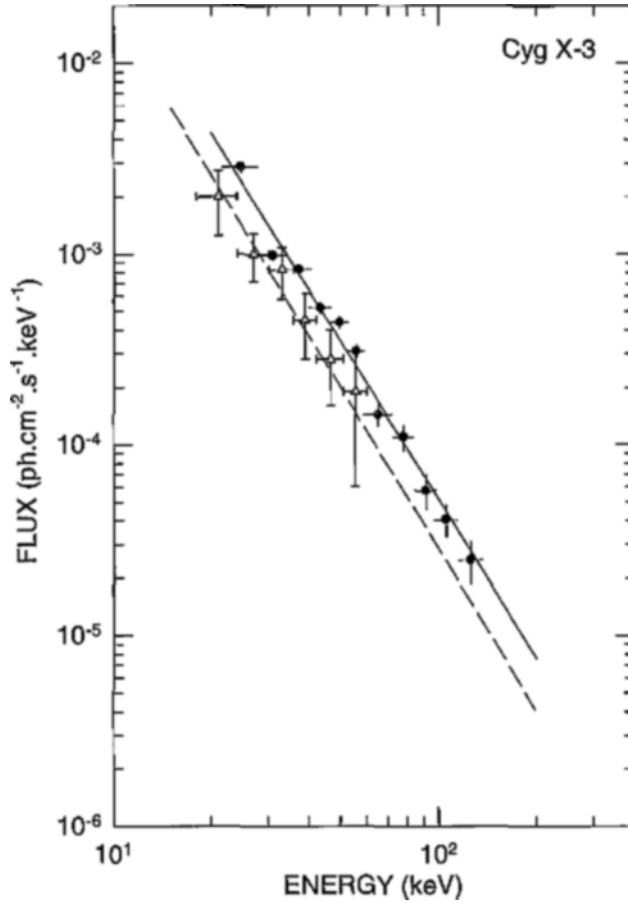


Figure 3. Hard X-ray spectra of Cyg X-3. The data of Rao *et al.* (1991) are shown for comparison (\triangle). The dotted line gives the best fit spectrum ($11.3 E^{-2.8}$) by the authors.

clear from Fig. 3 that both data agree completely both in magnitude and in the spectral shape. This comparison clearly supports the reliability of data presented in Fig. 2.

It is seen from Fig. 2, that the entire data can not be fitted to a simple mathematical function either with a single power law of the form $\frac{dN}{dE} = K E^{-\alpha}$ ph. cm⁻² s⁻¹ keV⁻¹ or a thermal spectrum of the type $\frac{A}{E}.e^{-E/kT}$. However above 40 keV the data can be reasonably represented by either of the two forms. The best fit model parameters for a 'forced fit' with single power law are $K = 1.8 \pm 0.2 \times 10^{-1}$ and $\alpha = 1.95 \pm 0.2$ for $\chi^2 \sim 2.3$ per degree of freedom thereby suggesting a composite fit. The spectral index of 1.95 ± 0.2 compares well with that of 'X-ray low' state value of ~ 2.1 (Ubertini *et al.* 1991, Ling *et al.* (1997) and is not surprising as the source was observed to be in the X-ray low/hard state since October 1996

(RXTE archival data). Similarly, a simple exponential function with a $kT \approx 35$ keV can be fitted to the data above 40 keV with a poor χ^2 value and the temperature compares well with the value of $kT = 36 \pm 6$ keV reported by Ubertini *et al.* (1991). No acceptable fit to the entire data was found even for a composite two component spectrum. A combined mathematical function with two temperatures fitted to the data is shown in Fig. 2 for illustration. The composite fit parameter values are $A_1 \sim 12$ kT ~ 3.54 keV, $A_2 \sim 7.3 \times 10^{-2}$ and kT value of 52 keV for a χ^2 value of 4.7. Similarly the best attempt with two component power law fit to the data corresponded to spectral indices of $\alpha_1 = 1.76 \pm 0.06$ and $\alpha_2 = 2.76 \pm 0.1$ and with the roll over energy $E_r \sim 26 \pm 2$ keV. The estimated luminosity of the source in the 20–200 band at the time of present observations is 2×10^{36} ergs/sec, assuming a source distance of 10 kpc.

In order to pinpoint the cause of disparity between the present measurements and the earlier data and its possible relation to its binary nature, we have plotted the binary light curve of Cyg X-1 in Fig. 3. The data shown in the lower panel are taken from Pooley *et al.* (1999) who have made a comparative study of orbital modulation in the X-ray and radio bands. The top panel corresponds to the phasogram computed from the BATSE daily average intensity of the source along with the present observation. For computing the 5.6^d phase, we have used the spectroscopic ephemeris of $P = 5^d.599847 \pm 0^d.000018$ and $T = \text{JD } 2441874.703 \pm 0.009$ (Brocksopp *et al.* 1999). It is seen from Fig. 4, that the epoch of our observation $\phi_{5.6} = 0.91$ does correlate to the minimum in the ASM light curve. Since the daily average intensity of the source obtained from the BATSE data does not show any large variation during the binary cycle of present observation and the average flux is higher by a factor of 5, we conclude that there may be a partial eclipsing of the hard X-ray emission region around the source. As discussed later, the knee-shaped spectral profile in the hard X-ray region is consistent with this conclusion. This feature might have been missed in the past experiments due to long integration intervals used to derive hard X-ray spectra because of the low sensitivity of the detector systems. High sensitivity of the present instrument allows snap-shot spectra of the bright X-ray sources with high statistical significance.

The wide band X-ray spectrum of Cygnus X-1 in the energy range 2–500 keV is very complex and requires multiple functions to fit the different sub-sets of the data and gives an acceptable value of χ^2 . Cui *et al.* (1997) have fitted the high state spectrum with a black body, broken power law and a high energy cut-off, while Chitnis *et al.* (1998) obtained the best χ^2 value with the addition of reflection component and an ad hoc edge at 7.76 keV. In these models the black-body component with $kT \sim 0.3$ keV accounts for 35% of the observed flux in the 2–10 keV band. A variety of physical models for black hole candidate X-ray sources describing the dynamical and thermodynamical properties of mass accretion like advection dominated accretion flow, Comptonization due to bulk motion, super Keplerian boundary layers and sub Keplerian mass flow, on to the compact objects have been discussed in literature (Narayan & Yi 1994; Titarchuk 1994; Chakrabarti & Titarchuk 1995). In the case of Cyg X-1, the X-ray photons are believed to orig-

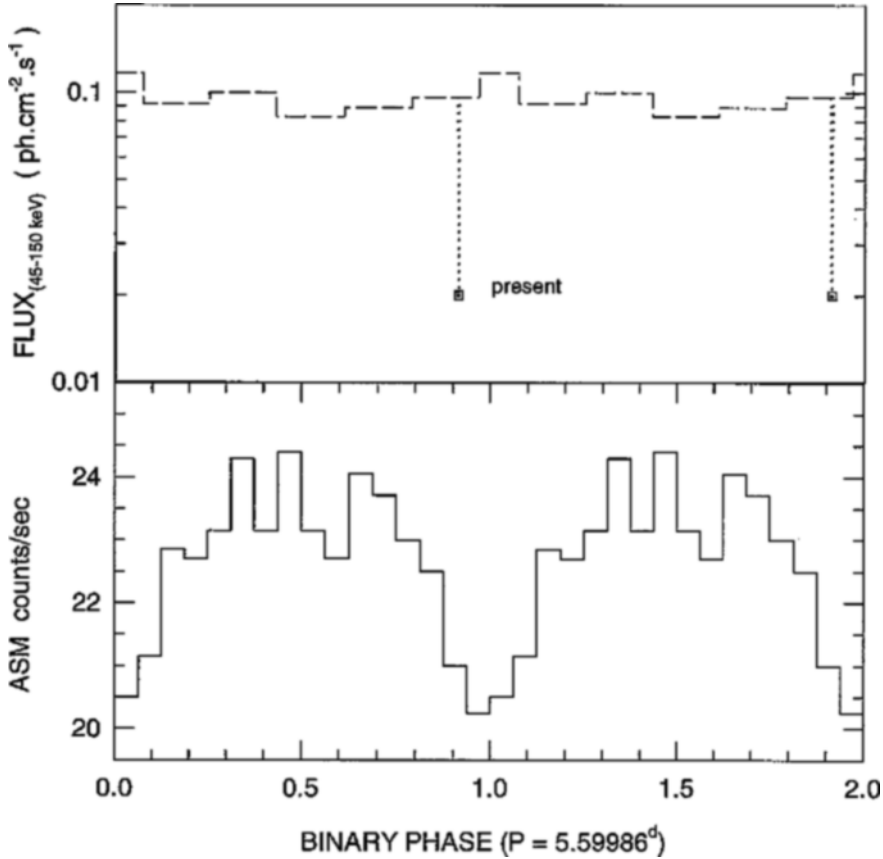


Figure 4. Binary phase histogram for Cyg X-1. See text for details

inate in two different sites. The low energy photons below 10 keV are emitted in optically thick accretion disk, while the hard X-ray photons originate in the Inverse Compton scattering process of the low energy photons in the hot corona around the X-ray object (Sunyaev & Titarchuk 1980, Liang & Nolan 1984). In order to fit the X-ray high/soft (γ_2) state, a two temperature concentric spherical geometry is adopted for the corona models, in which the photons between 25 and 300keV originate in the outer corona and the inner core contributes photons between 25 keV and 2 MeV (Skibo & Dermer 1995; Ling *et al.* 1997).

In a hot plasma, multiple scattering will control the energy exchange between electron and photon only if the plasma is very tenuous, since the bremsstrahlung and recombination losses are $\propto \rho^2$ and Thompson scattering goes as $\propto \rho$; where ρ is the number density. If $4kT_e > h\nu$, the seed photons will be upgraded in energy. Even for a Maxwellian distribution of electrons with $kT_e \ll m_e c^2$, the energy shift during each collision is given by $\frac{\nu'}{\nu} \sim 1 + \frac{4}{3}[\gamma^2 - 1]$. Therefore, multiple

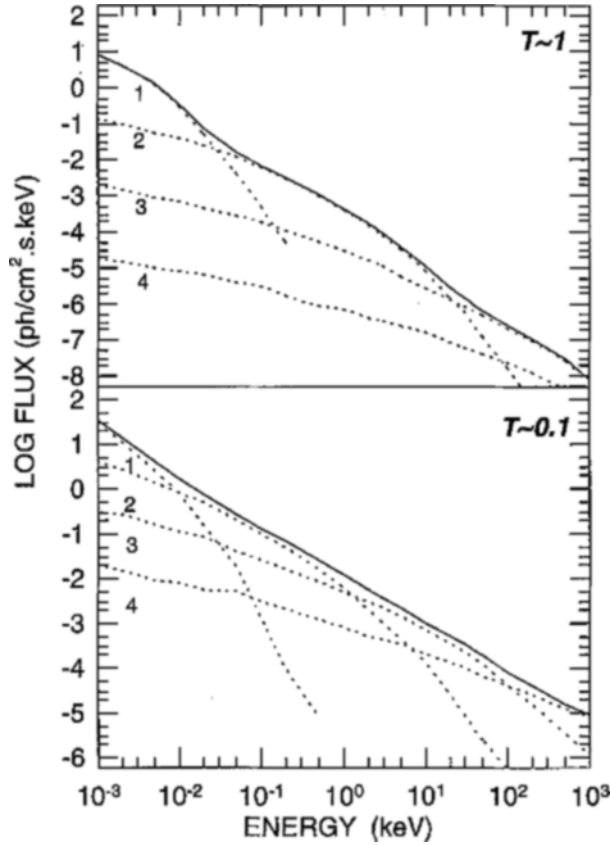


Figure 5. Sample curves for Comptonization of low energy photons in a cloud of weekly relativistic plasma for two values of optical depths and differing number of scattering.

scattering even by a Maxwellian gas can lead to very high photon energies. In a non-relativistic plasma where $kT_e \ll m_e c^2$ and $\tau \gg 1$, the average number of scattering for the seed photon $n_s \sim \tau^2$ and the probability density for multiple scattering is given as; $P(n_s) \propto \exp[\frac{n_s \pi^2}{3(\tau + \frac{2}{3})^2}]$. The emergent spectrum therefore, develops into a unified power law from the ensemble of spectra produced by the photons scattered by differing number of times. Both analytical and Monte-Carlo solutions for the spherical cloud and disk-shape geometry have been discussed in literature in relation to Cyg X-1 (Shapiro 1973; Sunyaev & Titarchuk 1980, Pozdnyakov *et al.* 1983, Hua & Titarchuk 1995) In the disk shape medium the output spectrum is a power law for $h\nu \sim kT_e$ and above $h\nu \gg kT_e$ it can be represented by Wein's distribution function given as $(\frac{h\nu}{kT_e})^3 \cdot e^{-h\nu/kT_e}$. A sample computation of Comptonization of the low energy photons in a weekly relativistic plasma for two values of optical depth is shown in Fig. 5. The dotted curves give the individ-

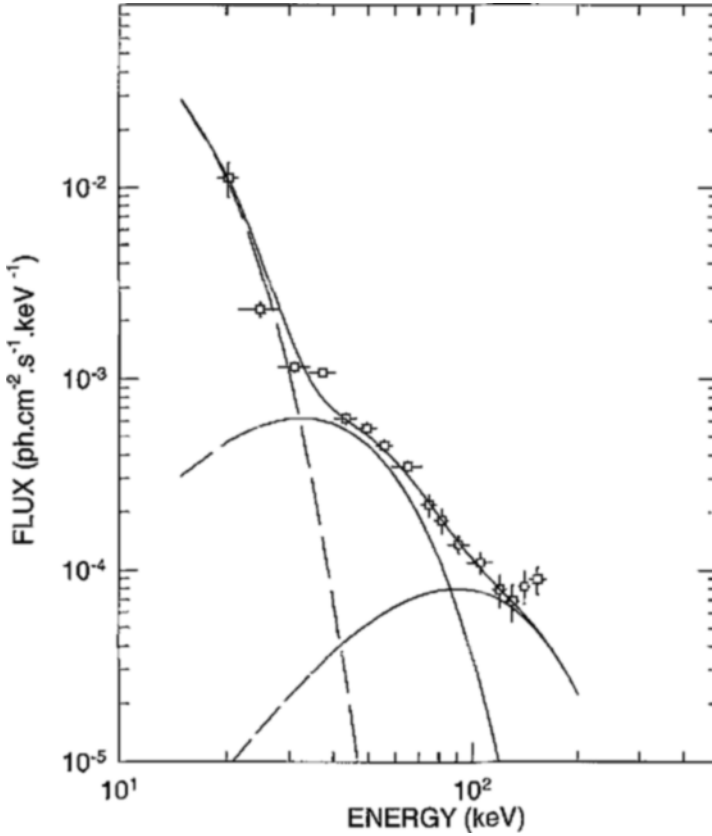


Figure 6. The spectral fit to the present data with multi-component Wien distribution function. Individual curves correspond to kT value of 2.8, 11.8 and 30 keV respectively.

ual contribution due to events with differing scattering number (Pozdnyakov *et al.* 1983).

It is clear from Fig. 5, that in the absence of any one of the individual components, the resultant spectrum will exhibit a sudden dip in the corresponding energy band. Therefore, in the physical model of hard X-ray generation due to Comptonization of the seed photons, it is possible to synthesize knee-shaped spectral profile by preferred selection of photon species, which have undergone differing number of scattering collisions. In a hot plasma with $kT_e = 27$ keV, an input seed photon with 1 keV energy requires about 20 scatterings to reach the maximum value of $3kT_e = 81$ keV.

It is therefore suggestive that the spectral shape seen in the present measurement is an ensemble with missing spectral components in which the input photons have gone through less number of scatterings. This can arise in an eclipsed geometry of the emitting region, where a part of the photons in the forward cone are

blocked and only albedo photons with a large average scattering angle are seen in the visibility cone. A large average scattering angle should in turn only arise in large number of scatterings. Fig. 5 shows the observed data fitted with a three component Wien spectrum. The best-fit parameters correspond to the kT value of 2.8, 11.8 and 30 keV. It is seen from the figure that multi-component Wien's function gives a very close fit to the data. The highest plasma temperature inferred from the present fit agrees well with the best fit kT_e value of 26.5 keV inferred by Sunyaev & Titarchuk (1980) in their original paper and derived temperatures during the X-ray low/hard state.

4. Summary

In this paper we have presented hard X-ray observations of Cyg X-1 which are radically different than the earlier measurements. Orbital analysis shows that the present data were taken in the minimum phase and the observed low flux indicates a possible partial eclipse of the hard X-ray emission region. The observed spectrum has a knee-shaped profile and can arise by selective summation of the multiple components in a physical model in which the hard X-ray emission arises due to Inverse Compton scattering of the seed photons.

Acknowledgements

I thank J. A. R. D'Silva, P. P. Madhwani, N. V. Bhagat, B. G. Bagade and Ms. N. Kamble for their support in fabrication of the payload and flight support. I also thank the staff at the TIFR balloon facility, Hyderabad for fabricating the balloon and conducting a successful balloon flight. BATSE and the RXTE instrument teams are thanked for making the data available on public archives.

References

- Brocksopp, C., Tarasov, A. E., Lyuty, V. M., Roche P., 1999, *Astron. Astrophys.*, **455**, 623.
Chitnis, V. R., Rao, A. R. & Agrawal P. C., 1998, *Astron. Astrophys.*, **331**, 251.
Cui, W., Heindl, W. A., Rothschild, R. E., Zhang, S. N. Jahoda K. & Focke W., 1997, *Ap. J.*, **474**, L57.
Dolan, J. F., Crannel, C. J., Dennis, B., Frost, K., & Orwig L. E., 1979, *Ap. J.*, **230**, 551.
D'Silva, J. A. R., Madhwani, P., Tembhurne N. & Manchanda, R. K., 1998, *Nucl. Instr. Meth.*, **A 412**, 342.
Giles, D. R. & Bolton, C. T., 1982, *Ap. J.*, **260**, 240.
Hua, X. M. & Titarchuk, L., 1995, *Ap. J.*, **449**, 188.
Kemp, J., Barbour, M. S., Hanson, G. D., Terrell, D. & Walker E. N. , 1983, *Ap. J.*, **100**, L75:
Kemp, J. C., Kartskaya, E. A., Kumisiashvili, M. I., Lyutyi, V. M., Kharuzina T. S. & Cherepshechuk A. M., 1987, *Soviet Astronomy*, **31**, 170.

- Liang, E. P. & Nolan, P. L., 1984, *Space Sci. Rev.*, **38**, 353.
- Ling, J. C., Mahoney, W. A., Wheaton, Wm. A., Jacobson, A. S., Kaluziensky, L., 1983, *Ap. J.*, **275**, 307.
- Ling, J. C., Wheaton, W. A., Wallyn, P., *et al.*, 1997, *Ap. J.*, **484**, 375.
- Manchanda, R. K., 1983, *Astrophys. Space Sci.*, **91**, 435.
- Narayan, R. & Yi, I., 1994, *Ap. J.*, **428**, L 13.
- Phlips, B. F., Jung, G. V. & Leising M. D. *et al.*, 1996, *Ap. J.*, **465**, 907.
- Pooley, G. G., Fender, R. P. & Brocksopp, C., 1999, *Mon. Not. R. Astr. Soc.*, **302**, L1.
- Pozdnyakov, L. A., Sobol I. M. & Sunyaev R. A., 1983, *Space Sci. Rev.*, **2**, 189.
- Priedhorsky, W. C. & Terrel, J. & Holt, S. S., 1983, *Ap. J.*, **270**, 233.
- Rao, A. R., Agrawal, P. C. & Manchanda, R. K., 1991, *Aston. Astrophys.*, **241**, 127.
- Shapiro, S. L., 1973, *Ap. J.*, **180**, 531.
- Skibo, J. G., Dermer, C. D., 1995, *Ap. J.*, **455**, L25.
- Sunyaev, R. A. & Titarchuk L. G., 1980, *Astron. Astrophys.*, **86**, 121.
- Tanaka, Y. 1989, in Proc. 23rd ESLAB Symposium on Two Topics in X-ray Astronomy, ed. J. Hunt & B. Battrock (Paris: ESA), 3
- Tanaka, Y. & Lewin, W. H. G., 1995, in X-ray Binaries, ed. W. H. G. Lewin, J. van Paradijs & E. P. J. van den Heuvel, Cambridge Uni. Press, 126.
- Titarchuk, L. G., 1994, *Ap. J.*, **434**, 570.
- van der Klis, M. , 1995, in X-ray Binaries, ed. W. H. G. Lewin, J. van Paradijs, & E. P. J. van den Heuvel, Cambridge Uni. Press, 126.
- Ubertini, P., Bazzano, A., La Padula, C., Manchanda, R. K. & Polcaro, V. F., 1991, *Ap. J.*, **383**, 263.